ISSN 1392 - 1207. MECHANIKA. 2012 Volume 18(2): 186-191

Flexural vibration band gaps in periodic stiffened plate structures

Jianwei Wang, Gang Wang, Jihong Wen, Xisen Wen
Institute of Mechatronical Engineering, National University of Defense Technology, Changsha, 410073, China, E-mail: wenxs@vip.sina.com
Key Laboratory of Photonic and Phononic Crystal, Ministry of Education, Changsha, 410073, China
crossref http://dx.doi.org/10.5755/j01.mech.18.2.1557

1. Introduction

Due to their high rigidity-to-weight ratio and economical cost, stiffened plate and shell structures are used extensively in various engineering applications such as bridges, ship hulls and decks, and aircraft structures. In the past few decades, many researchers have discussed the performance of stiffened plates under dynamic loading, which may lead to a wide implementation in the field of vibration and noise control. Determining the free vibration characteristics of a structural system is a fundamental task in dynamic analysis.

Recently, the propagation of elastic or acoustic waves in artificial periodic composite structures known as phononic crystals (PCs) has received a great deal of attention [1-4]. One of the most attractive characteristics of PCs is that the propagation of sound and other vibrations is forbidden in their elastic wave band gaps. PCs are essentially periodic structures, and they have inherent relations with periodic structures widely used in traditional engineering. Introducing the theoretical and calculation methods of PCs into the investigation of the dynamic behavior of periodic structures in engineering will provide a new technique for the control of vibration and noise. So far, vibration band gaps in periodic beam [5], grid [6, 7], and plate [8] structures have been researched. These studies are theoretically significant, but the structures studied are less practical than those structures widely used in engineering, such as stiffened plate structures. Moreover, the theoretical methods for calculating the band gaps of PCs such as the plane wave expansion (PWE) method, the Finite-difference-time-domain (FDTD) method, the multiple-scattering theory (MST) method, and the lumped-mass method, are valid for a periodic beam or plate structure. However, by using the above methods, it is difficult to calculate the band gaps of more complicated engineering structures, such as the stiffened plate.

In the late 1980s, Mead and his collaborators[9] studied propagating wave motion in regularly stiffened plates and stiffened cylindrical shells using the hierarchical finite element method. Mead et al. [10] modelled the beams as simple line supports and analysed free vibration of an orthogonally stiffened flat plate. Later, they [11, 12] also determined the propagation frequencies of elastic waves by computing phase constant surfaces for a number of different cylinder-stiffener configurations. Cheng Wei and Zhu Dechao [13] analysed the characteristics of wave propagation in a periodic plate reinforced by regular orthogonal stiffeners and discussed the effect of the ratio of length to width, the parameters of the stiffeners, and boundary conditions.

However, there are two main problems with these studies. First, the stiffened plate structures must be divided into small finite elements to ensure that the stiffeners are always located on the boundaries of these elements. As a result, the number of the finite elements will dramatically increase as the number of stiffeners with different orientations increases or those with a small spacing between them increases. Second, the theory to predict the vibration response of the stiffened plate structures has been primarily applied to analyse periodic structures as pass band and stop band. However, the physical mechanism of the band gaps has not been exhaustively explained [9].

The present work presents an improved finite element model for periodic stiffened plate structures with any number or orientation of stiffeners. Using the model, we analyse flexural vibration band gaps and study the physical mechanism for their formation in these periodic structures.

This paper is organized as follows. In section 2, we summarized the fundamentals of the technique used to analyse the propagation of waves in 2-D periodic structures. Moreover, we established a finite element model of the stiffened plate by considering the unit cell of the infinite periodic structure discussed. Within the model, any number of stiffeners is allowed to take on an arbitrary orientation, and they need not necessarily follow the nodal lines of the mesh division. In section 3, the flexural vibration band gaps of the periodic grid structure and the periodic stiffened plate structures with different skin thicknesses are calculated and comparatively analysed. Finally, the main conclusions of this work are discussed in section 4.

2. Finite element description

2.1. Analysis of free wave motion

A generic 2-D periodic structure is assembled by identically connecting a base unit or cell along the x-y plane. According to Bloch's theorem, a wave propagating in a 2-D periodic structure can be described by the motion of a single cell and by a propagation vector defining the wave amplitude and phase change from one cell to the next [14]. A schematic of the stiffened plate structure configuration and associated unit cell is shown in Fig. 1.

Wave motion in the 2-D periodic structure can be expressed as follows

$$\boldsymbol{w}(\boldsymbol{r},\boldsymbol{n}) = \boldsymbol{w}_0 e^{\boldsymbol{\mu}\cdot r} \tag{1}$$

where $\boldsymbol{w}$ is the generalized displacement of point $\boldsymbol{r}$ belonging to the unit cell at location $\boldsymbol{n}$, while $\boldsymbol{w}_0$ describes the

motion of the unit cell. Also, $\boldsymbol{\mu}=\begin{bmatrix}\mu_x & \mu_y\end{bmatrix}$ is the vector of the propagation constants. The propagation constants are complex numbers and control the nature of elastic wave propagation in the 2-D periodic structure.

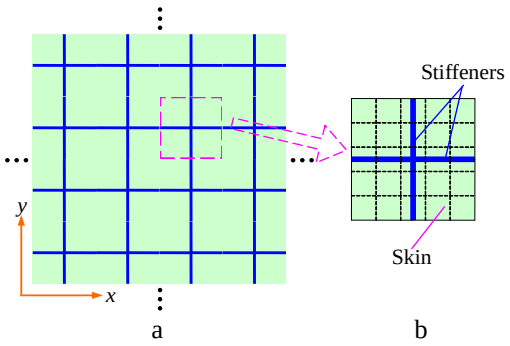

Fig. 1 a - schematic of the periodic stiffened plate structure; b - corresponding unit cell

The behaviour of the unit cell can be conveniently described by defining the cell's interaction with its neighbours and using a discretized equation of motion. For plane harmonic waves at frequency ω, the equation of motion for the unit cell can be written as

$$\left(\boldsymbol{K}-\omega^2\boldsymbol{M}\right)\boldsymbol{\delta}=\boldsymbol{F} \tag{2}$$

where the matrices $\boldsymbol{K}$ and $\boldsymbol{M}$ denote the assembled global stiffness and mass matrix of the unit cell respectively. The vectors $\boldsymbol{\delta}$ and $\boldsymbol{F}$ are the nodal displacements and forces respectively.

From Bloch's theorem, the following relationships are obtained for the unit cell interfaces [7, 15]

$$\left.\begin{aligned}
&\boldsymbol{\delta}_r=e^{\mu_x}\boldsymbol{\delta}_l,\ \boldsymbol{\delta}_t=e^{\mu_x}\boldsymbol{\delta}_b,\\
&\boldsymbol{\delta}_{lt}=e^{\mu_y}\boldsymbol{\delta}_{lb},\ \boldsymbol{\delta}_{rb}=e^{\mu_y}\boldsymbol{\delta}_{lb},\ \boldsymbol{\delta}_{rt}=e^{\mu_x+\mu_y}\boldsymbol{\delta}_{lb}\\
&\boldsymbol{F}_r=-e^{\mu_x}\boldsymbol{F}_l,\ \boldsymbol{F}_t=-e^{\mu_y}\boldsymbol{F}_b,\\
&\boldsymbol{F}_{rt}+e^{\mu_x}\boldsymbol{F}_{lt}+e^{\mu_y}\boldsymbol{F}_{rb}+e^{\mu_x+\mu_y}\boldsymbol{F}_{lb}=0
\end{aligned}\right\} \tag{3}$$

where the subscripts *l*, *r*, *b*, *t*, *rb*, *lb*, *rt*, *lt*, and *i* respectively indicate the generalized displacements at the left, right, bottom, top, right-bottom, left-bottom, right-top, left-top, and internal nodes of the unit cell, as shown in Fig. 2.

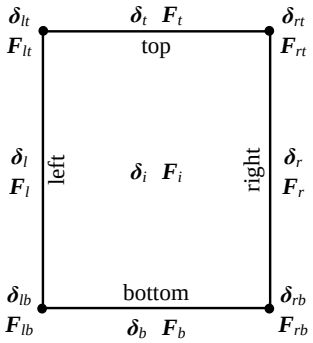

Fig. 2 A generic unit cell for a two-dimensional periodic structure

Using the above relationships, one can define the following transformation

$$\boldsymbol{\delta}=\boldsymbol{T}_1\boldsymbol{\delta}_{red} \tag{4}$$

where $\boldsymbol{\delta}_{red}$ denotes the displacement of the nodes in the Bloch reduced coordinates defined by

$$\boldsymbol{\delta}_{red}=\begin{bmatrix}\boldsymbol{\delta}_i & \boldsymbol{\delta}_b & \boldsymbol{\delta}_l & \boldsymbol{\delta}_{lb}\end{bmatrix}^T \tag{5}$$

and T_1 is a linear transformation parameterized by μ_x and μ_y.

For free wave motion, Eq. (2) would be written as

$$\left(\boldsymbol{K}_{red}-\omega^2\boldsymbol{M}_{red}\right)\boldsymbol{\delta}_{red}=\boldsymbol{T}_1^H\boldsymbol{F}=0 \tag{6}$$

where the superscript *H* denotes the Hermitian transpose and $\boldsymbol{K}_{red}$ and $\boldsymbol{M}_{red}$ are the reduced stiffness and mass matrices according to Bloch's theorem and defined by

$$\boldsymbol{K}_{red}=\boldsymbol{T}_1^H\boldsymbol{K}\boldsymbol{T}_1,\ \ \boldsymbol{M}_{red}=\boldsymbol{T}_1^H\boldsymbol{M}\boldsymbol{T}_1 \tag{7}$$

Eq. (7) is the desired eigenvalue problem parameterized by ω and defines the dispersion relations of the infinite periodic structure.

2.2. Finite element modeling of the unit cell

The unit cell of an infinite periodic stiffened plate structure consists of a base structure forming the "skin" as well as local reinforcement elements called "stiffeners" which are periodically collocated. Therefore, based on Mindlin plate theory and Timoshenko beam theory, the dynamic characteristic of the unit cell can be accurately described by establishing an efficient finite element model of the stiffened plate using eight-node isoparametric plate bending elements and three-node isoparametric beam elements.

According to the Mindlin plate theory, the stiffness and mass matrices of the eight-node isoparametric plate bending element are given [16, 17] by

$$\left.\begin{aligned}
\boldsymbol{K}_p&=\iint\boldsymbol{B}_p^T\boldsymbol{D}_p\boldsymbol{B}_p dxdy=\int_{-1}^{1}\int_{-1}^{1}\boldsymbol{B}_p^T\boldsymbol{D}_p\boldsymbol{B}_p\,det|\boldsymbol{J}|d\xi d\eta\\
\boldsymbol{M}_p&=\iint\boldsymbol{N}_p^T\boldsymbol{m}_p\boldsymbol{N}_p dxdy=\int_{-1}^{1}\int_{-1}^{1}\boldsymbol{N}_p^T\boldsymbol{m}_p\boldsymbol{N}_p\,det|\boldsymbol{J}|d\xi d\eta
\end{aligned}\right\} \tag{8}$$

where $\boldsymbol{J}$ is the Jacobian matrix, $\boldsymbol{B}_p$ is the strain-displacement relationship matrix, $\boldsymbol{D}_p$ is the constitutive matrix, $\boldsymbol{N}_p$ is the mapped shape functions of the plate element, and $\boldsymbol{m}_p$ is defined as

$$\boldsymbol{m}_p=\rho_p\begin{bmatrix}h_p & 0 & 0\\ 0 & h_p^3/12 & 0\\ 0 & 0 & h_p^3/12\end{bmatrix} \tag{9}$$

where ρ_p is the density of the plate material and h_p is the thickness of the plate element.

The Timoshenko beam element has three nodes and each node has three degrees of freedom, (w_b, θ_{bs}, θ_{bt}). The stiffness and mass matrices of the isoparametric beam element are then given by

$$\left.\begin{aligned}
\boldsymbol{K}_b&=\int\boldsymbol{B}_b^T\boldsymbol{D}_b\boldsymbol{B}_b ds=\int_{-1}^{1}\boldsymbol{B}_b^T\boldsymbol{D}_b\boldsymbol{B}_b|\boldsymbol{J}|d\xi'\\
\boldsymbol{M}_b&=\int\boldsymbol{N}_b^T\boldsymbol{m}_b\boldsymbol{N}_b ds=\int_{-1}^{1}\boldsymbol{N}_b^T\boldsymbol{m}_b\boldsymbol{N}_b|\boldsymbol{J}|d\xi'
\end{aligned}\right\} \tag{10}$$

where $\boldsymbol{B}_b$ is the strain-displacement relationship matrix, $\boldsymbol{D}_b$ is the constitutive matrix, $\boldsymbol{N}_b$ is the mapped shape functions of the beam element, and $\boldsymbol{m}_b$ is defined as

$$\boldsymbol{m}_b = \rho_b \begin{bmatrix} A_b & 0 & 0 \\ 0 & I_{bz} & 0 \\ 0 & 0 & J_b \end{bmatrix} \tag{11}$$

where ρ_b is the density of the beam material, A_b is the cross-sectional area of the beam, I_{bz} is the second moment of the beam cross-sectional area about the z-axis, and J_b is the polar moment of inertia of the beam.

The displacement field of the stiffener element is expressed using the plate element degrees of freedom [18, 19] as

$$\sum_{i=1}^{3} \{\delta_b\}_i = \boldsymbol{\Lambda} \boldsymbol{T}_2 \sum_{r=1}^{8} \{\delta\}_r \tag{12}$$

$$\boldsymbol{\Lambda} = \begin{bmatrix} \boldsymbol{\Lambda}_1 & & \\ & \boldsymbol{\Lambda}_2 & \\ & & \boldsymbol{\Lambda}_3 \end{bmatrix}, \boldsymbol{\Lambda}_i = \begin{bmatrix} 1 & 0 & 0 \\ 0 & \cos\varphi & \sin\varphi \\ 0 & -\sin\varphi & \cos\varphi \end{bmatrix} \tag{13}$$

$$\boldsymbol{T}_2 = \sum_{i=1}^{3} \sum_{r=1}^{8} \left(N_r \boldsymbol{I}\right)_i \tag{14}$$

where $\boldsymbol{\Lambda}$ is the orientation matrix, φ is the stiffener inclination with respect to the plate x-axis, $\boldsymbol{T}_2$ is the transformation matrix of the nodal displacements from the beam element nodes into the plate element nodes, and $(N_r \boldsymbol{I})_i$ (i = 1, 2, 3) are the shape functions of the eight-node plate elements defined at the 3 points (m, n, p) in the ξ-η coordinate system, as shown in Fig. 3. The stiffener node coordinates in the ξ-η coordinate system are obtained using the plate shape functions themselves, and the solution can easily be calculated using Newton's iteration method.

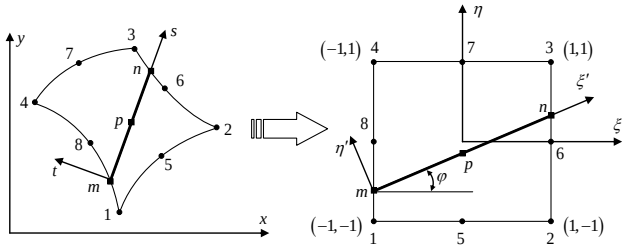

Fig. 3 Mapping of the stiffened plate element from the global coordinate system to the local coordinate system

Furthermore, the stiffness and mass matrices of a stiffener element can be expressed in terms of the plate nodal degrees of freedom as

$$\left.\begin{aligned} \boldsymbol{K}_s &= \boldsymbol{T}_2^T \boldsymbol{\Lambda}^T \boldsymbol{K}_b \boldsymbol{\Lambda} \boldsymbol{T}_2 \\ \boldsymbol{M}_s &= \boldsymbol{T}_2^T \boldsymbol{\Lambda}^T \boldsymbol{M}_b \boldsymbol{\Lambda} \boldsymbol{T}_2 \end{aligned}\right\} \tag{15}$$

Finally, the combined stiffness and mass matrices of the stiffened plate for the unit cell are calculated by adding those of the plate elements and of the stiffener elements. Using above approach, any number or orientation of stiffeners within the unit cell can be easily modelled without the need to change the ground mesh of the plate.

3. Results and discussion

3.1. Flexural vibration band gaps of periodic grid structures

In order to compare with the flexural vibration band gap characteristics of periodic stiffened plate structures, it is necessary to analyse the characteristics of periodic grid structures.

The grid structure has the same geometry and material properties of the stiffened plate structures but does not have the same skin. The material parameters used are ρ_{steel} = 7780 kg/m^3, E_{steel} = 21.06×10^{10} Pa and v_{steel} = 0.3. The lattice constant of the unit cell is 0.25 m, and the grid section parameters are b = 0.015 m and h = 0.015 m. The flexural vibration band structure of the grid structure using the above finite element method (FEM) is shown in Fig. 4, a. It is well known that the frequency response function (FRF) of vibration can be used to effectively describe the band gaps. The FRF of the flexural vibration was determined with the FEM software, MSC Nastran, for a 16×16 grid and is illustrated in Fig. 4, b. There are no complete band gaps in the band structure or any large attenuation in the FRF.

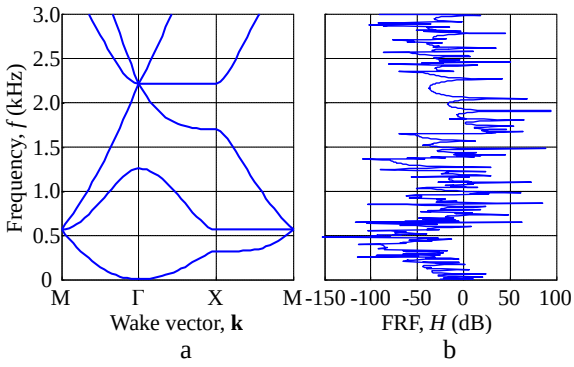

Fig. 4 a - flexural wave band structure of the periodic grid structure, b - corresponding FRF

3.2. The influence of the skin thickness on flexural vibration band gaps of periodic stiffened plate structures

The material parameters of the skin in the periodic stiffened plate structures are ρ_{epoxy} = 180 kg/m^3, E_{epoxy} = 4.35×109 Pa, v_{epoxy} = 0.3679, and d_{epoxy} = 0.02. The thickness parameters of the skin are varied to analyse the influence of the skin thickness on flexural vibration band gaps of the periodic stiffened plate structures.

Fig. 5 shows the flexural vibration band structure and the finite structure FRF of the periodic stiffened plate structure with a 1 mm-thick skin. It can be clearly seen from the band structure in Fig. 5, a that there are numerous dispersion curves which are almost flat along all three boundaries of the irreducible Brillouin zone. The frequencies of the flat bands are approximately the eigenvalues of the localized vibration modes of the stiffener-surrounded skin (which can be considered a four-sides-clamped plate) especially in the 0~0.4 kHz region, as shown in Fig. 6.

An enlarged figure of the dashed rectangular region in Fig. 5, a is shown in Fig. 7. The mode shapes of the stiffeners and the skin corresponding to the four points

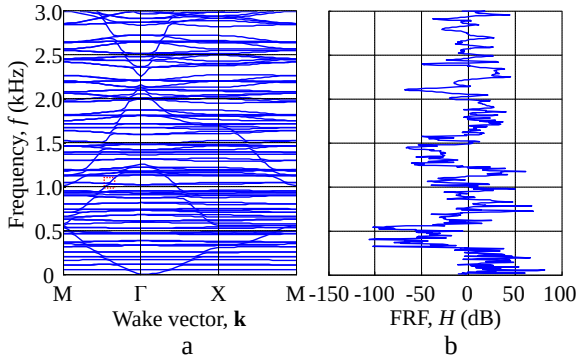

Fig. 5 a - flexural wave band structure of the periodic stiffened plate structure; the skin thickness is 1 mm; b - corresponding FRF

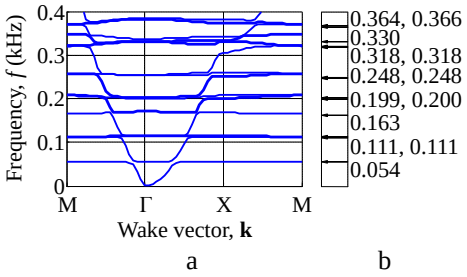

Fig. 6 a - flexural wave band structure of the periodic stiffened plate structure from 0~0.4 kHz; the skin thickness is 1 mm; b - natural frequencies of the four-sides-clamped plate

(marked as A, B, C, and D) of the dispersive curves in Fig. 7 are plotted in Fig. 8. It is clearly seen that the skin is in localized vibration modes and the flexural vibration displacement of the stiffeners is much smaller than that of the skins at A and B, although not at C or D. Hence, the curves are considered the same as the dashed lines shown in Fig. 7. In fact, if the flat bands are ignored, the dispersion curves for the system with a 1 mm-thick skin are quite similar to those of the periodic grid structure. In other words, the vibrations of the skin and the stiffeners are uncoupled, and the vibration of the stiffeners plays a major role in the stiffened plate system.

Similar to the periodic grid structure, there also is no complete band gap in the band structure or any large drop in the FRF.

The band structure and the FRF corresponding to the 8 mm-thick skin are shown in Fig. 9. Due to the increase of the skin to stiffener thickness ratio, the number of flat curves is relatively smaller in the range of 0 ~ 3 kHz and the four-sides-clamped boundary condition is weakened such that the curves are no longer flat. This means that the vibration coupling between the skin and the stiffeners is strengthened. Moreover, there are large drops in the FRF. The frequency ranges, 0.520 ~ 0.540 kHz, 0.786 ~ 1.351 kHz, and 1.781 ~ 2.740 kHz are labelled as I, II, and III and shown in Fig. 9, b. The first drop agrees with the first complete band gap (0.534 ~ 0.564 kHz) in band structure. There is a series of peaks within the other two large drops. These peaks are primarily a result of two phenomena. The first is that the vibration of the stiffeners couples with the skin and the amplitudes of the mode shapes of the skin and the stiffeners are both larger. For example, the mode shapes of the skin and the stiffeners at points marked E and F are shown in Fig. 10. The second is that the FRF is not that of an infinite periodic structure. The results measured at the 14th period and the 16th period of the 16×16 structure are shown in Fig. 9, b as the dashed line and the solid line respectively. It is clearly seen that the attenuation at the 14th period is larger than that at the 16th period. That is to say, the effect of boundary condition of finite structure at the 14th period is smaller than that at the 16th period.

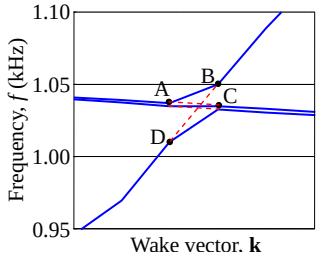

Fig. 7 The enlarged drawing of the specified dashed rectangular region in Fig. 5, a

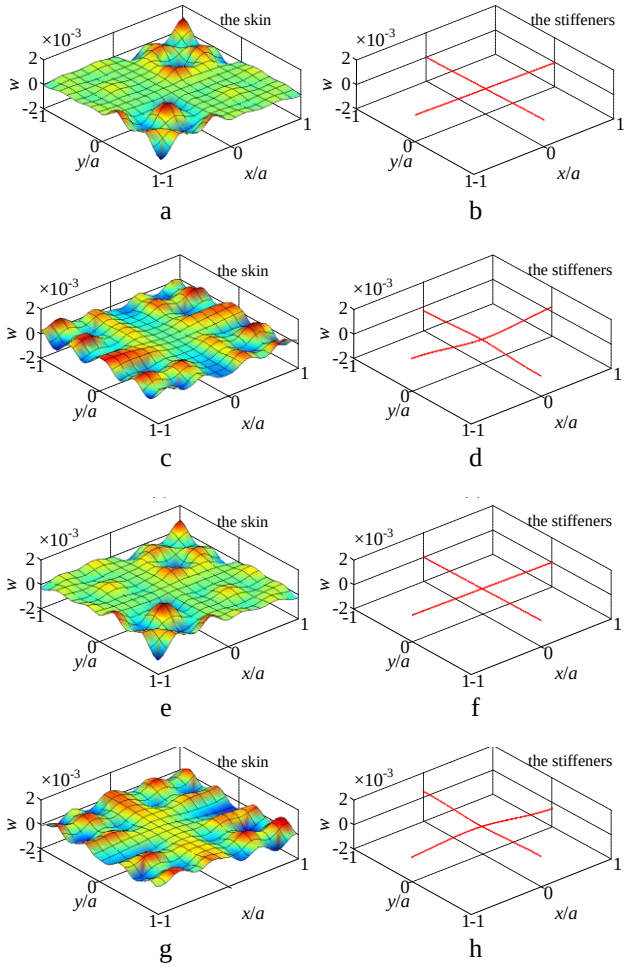

Fig. 8 The mode shapes of the skin and the stiffeners: a and b refer to point A; c and d refer to point B; e and f refer to point C; and g and h refer to point D in Fig. 7

The corresponding results of the stiffened plate structure, which show that the thickness of the skin is the same as those of the stiffeners, are given in Fig. 11, a and c. The natural frequencies of the four-sides-clamped plate are plotted in Fig. 11, b. In this case, the boundary conditions for the four-sides-clamped plate are no longer applicable for the stiffeners-surrounded skin and all of the dispersive

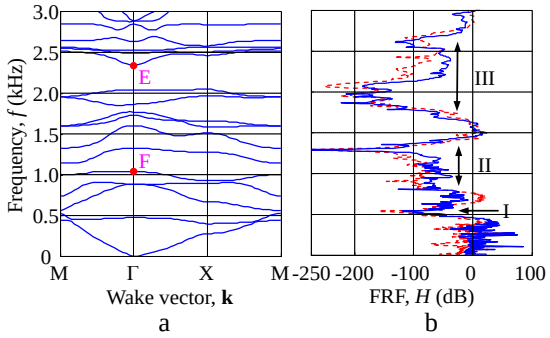

Fig. 9 a - flexural wave band structure of the periodic stiffened plate structure; the skin thickness is 8 mm; b - corresponding FRF

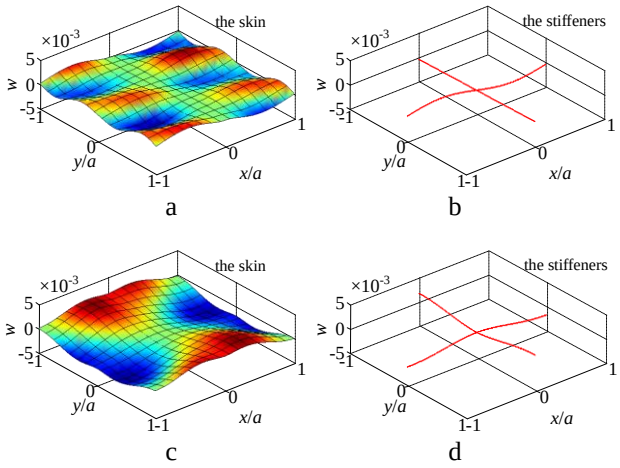

Fig. 10 The mode shapes of the skin and the stiffeners; a and b refer to point E, and c and d refer to point F in Fig. 9, a

curves are distinctly flexural. The vibrations of the skin and the stiffeners are strongly coupled. This is evidence that there is not a complete band gap in the band structure, and this conclusion can also be made from the FRF result.

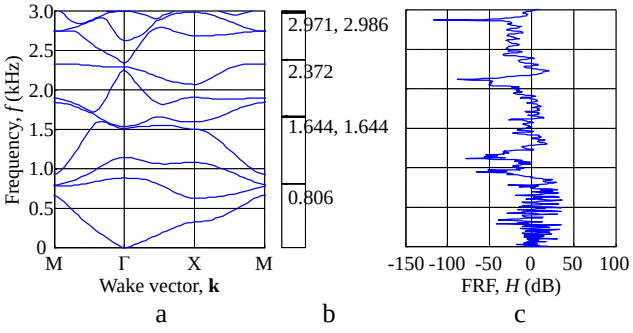

Fig. 11 a - flexural wave band structure of the periodic stiffened plate structure; the skin thickness is 15 mm; b - natural frequencies of the skin which is clamed along four sides; c - corresponding FRF

The flexural vibration band gaps of the stiffened plate structures in which the thickness of the skin varies from 1 mm to 15 mm are calculated, and the frequency ranges of the former six complete band gaps are plotted in Fig. 12. It can be seen that, while the skin to stiffener thickness ratio increases, several complete band gaps appear and when the thickness of the skin is close to that of the stiffener, the complete band gaps gradually disappear.

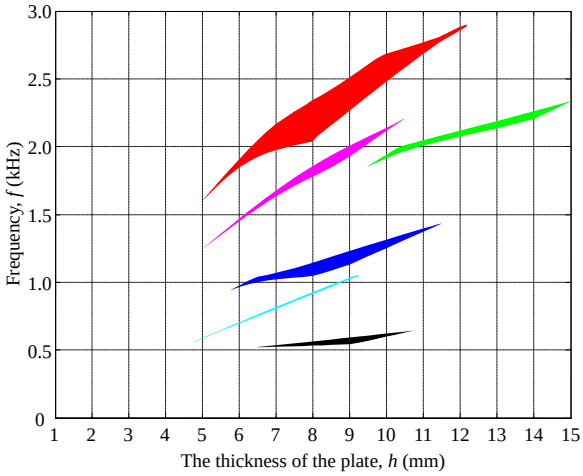

Fig. 12 Variation of the frequency ranges of the former six complete band gaps with skin thickness from 1 mm to 15 mm

4. Conclusion

An improved finite element model of the periodic stiffened plate structures is established and used to analyze flexural wave propagation in periodic stiffened plate structures. The model demonstrates that the skin and the stiffeners are vibration coupled. When the height of the cross section of the stiffeners is much larger than the thickness of the skin, the coupling between them is relatively weak and the stiffeners play a major role in the band gap characteristics of the stiffened-plate system. As the thickness ratio between the skin and stiffeners increases, the four-sides-clamped boundary condition weakens. Therefore, the vibration coupling between the skin and the stiffeners is strengthened and several complete band gaps are generated. These band gaps primarily correspond to the frequency ranges of vibration attenuation. When the thickness of the skin is equal to that of the stiffeners, the vibrations of the skin and the stiffeners are strongly coupled and the homogeneous skin weakens the impedance matching of the periodic stiffeners so that the complete band gaps vanish. These results show that the vibration coupling between the skin and stiffeners influence the formation of the complete band gap. By optimizing the thickness ratio of the skin and the stiffeners, large attenuation can be expected in various frequency ranges.

Acknowledgment

This work was supported by the National Natural Science Foundation of China (Grant No.50905182, 50875255) and the Foundation for the Author of National Excellent Doctoral Dissertation of China.

References

1. **Kushwaha, M.S.; Halevi, P.; Dobrzynski, L.; etc.** 1993. Acoustic band structure of periodic elastic composites, Phys. Rev. Lett. 71(13): 2022-2025. http://dx.doi.org/10.1103/PhysRevLett.71.2022.
2. **Sigalas, M.M.; Economou, E.N.** 1994. Elastic waves in plates with periodically placed inclusions, Journal of Applied Physics 75(6): 2845-2850. http://dx.doi.org/10.1063/1.356177.

3. **Liu Zheng You; Xi Xiang Zhang; Yi Wei Mao; etc.** 2000. Locally resonant sonic materials, Science 289: 1734-1736.
4. **Wang Gang; Xi Sen Wen; Ji Hong Wen; etc.** 2004. Two-dimensional locally resonant phononic crystals with binary structures, Phys. Rev. Lett. 93(15): 154302. DOI: 10.1103/PhysRevLett.93.154302.
5. **Wen Ji Hong; Gang Wang; Dian Long Yu; etc.** 2005. Theoretical and experimental investigation of flexural wave propagation in straight beams with periodic structures: Application to a vibration isolation structure, Journal of Applied Physics 97(11): 114907. doi.org/10.1063/1.1922068.
6. **Wen Ji Hong; Dian Long Yu; Jing Wen Liu; etc.** 2009. Theoretical and experimental investigations of flexural wave propagation in periodic grid structures designed with the idea of phononic crystals, Chinese Physics B 18(6): 2404-2411. http://dx.doi.org/10.1088/1674-1056/18/6/048.
7. **Srikantha Phani, A.; Woodhouse, J.; Fleck, N.A.** 2006. Wave propagation in two-dimensional periodic lattices, The Journal of the Acoustical Society of America 119(4): 1995-2005. http://dx.doi.org/10.1121/1.2179748.
8. **Yu Dian Long; Yao Zong Liu; Ji Hong Wen; etc.** 2006. Flexural vibration band gaps in two-dimensional periodic thick plates, in Proceedings of the 2nd International Conference on Dynamics, Vibration and Control, Beijing, China.
9. **Mead, D.M.** 1996. Wave propagation in continuous periodic structures: Research contributions from Southampton, 1964-1995, Journal of Sound and Vibration 190(3): 495-524. http://dx.doi.org/10.1006/jsvi.1996.0076.
10. **Mead, D.J.; Zhu, D.C.; Bardell, N.S.** 1988. Free vibration of an orthogonally stiffened flat plate, Journal of Sound and Vibration 127(1): 19-48. http://dx.doi.org/10.1016/0022-460X(88)90348-3.
11. **Bardell, N.S.; Mead, D.J.** 1989. Free vibration of an orthogonally stiffened cylindrical shell, Part I: Discrete line simple supports, Journal of Sound and Vibration 134(1): 29-54. http://dx.doi.org/10.1016/0022-460X(89)90735-9.
12. **Bardell, N.S.; Mead, D.J.** 1989. Free vibration of an orthogonally stiffened cylindrical shell, Part II: Discrete general stiffeners, Journal of Sound and Vibration 134(1): 55-72. http://dx.doi.org/10.1016/0022-460X(89)90736-0.
13. **Cheng Wei; De Chao Zhu** 1994. The characteristics of wave propagation in a periodic orthogonally stiffened flat plate, Acta Mechanica Sinica 26(3): 297-302.
14. **Brillouin Leon** 1953. Wave Propagation in Periodic Structures: Electric Filters and Crystal Lattices, New York, Dover Publications.
15. **Farzbod Farhad; Michael J. Leamy** 2009. The treatment of forces in Bloch analysis, Journal of Sound and Vibration 325(3): 545-551. http://dx.doi.org/10.1016/j.jsv.2009.03.035.
16. **Prusty, B.G., Satsangi, S.K.** 2001. Analysis of stiffened shell for ships and ocean structures by finite element method, Ocean Engineering 28(6): 621-638. http://dx.doi.org/10.1016/S0029-8018(00)00021-4.
17. **Akl, W.; El-Sabbagh, A.; Baz, A.** 2008. Optimization of the static and dynamic characteristics of plates with isogrid stiffeners, Finite Elements in Analysis and Design 44(8): 513-523. http://dx.doi.org/10.1016/j.finel.2008.01.015.
18. **Thompson, P.A., Bettess, P.; Caldwell, J.B.** 1988. An isoparametric eccentrically stiffened plate bending element, Engineering Computations 5(2): 110-116. http://dx.doi.org/10.1108/eb023728.
19. **Ojeda, Roberto; Gangadhara Prusty, B.; Lawrence, Norman; etc.** 2007. A new approach for the large deflection finite element analysis of isotropic and composite plates with arbitrary orientated stiffeners, Finite Elements in Analysis and Design 43: 989-1002. http://dx.doi.org/10.1016/j.finel.2007.06.007.

Jianwei Wang, Gang Wang, Jihong Wen, Xisen Wen

LENKIMO SVYRAVIMŲ DAŽNIO JUOSTŲ TRŪKIAI PERIODIŠKAI SUSTANDINTŲ PLOKŠČIŲ KONSTRUKCIJOSE

R e z i u m ė

Remiantis Mindlino plokščių ir Timošenko sijų teorijomis bei Blohso teorema sukurtas patikslintas baigtinių elementų modelis tampriųjų bangų sklidimui lenkimo svyravimų veikiamose periodiškai sustandintų plokščių konstrukcijose su bet kokiu skaičiumi bet kaip orientuotų standumo elementų apskaičiuoti. Naudojant baigtinių elementų modelį palyginti ir išanalizuoti lenkimo svyravimų dažnių juostos trūkiai periodinių tinklų konstrukcijose ir įvairiose periodiškai sustandintų plokščių konstrukcijose su skirtingo storio dangomis. Rezultatai rodo, kad dangos ir standumo elementų svyravimų sąveika turi įtakos lenkimo svyravimų dažnio juostų trūkimui.

Jianwei Wang, Gang Wang, Jihong Wen, Xisen Wen

FLEXURAL VIBRATION BAND GAPS IN PERIODIC STIFFENED PLATE STRUCTURES

S u m m a r y

Based on Mindlin plate theory, Timoshenko beam theory and Bloch's theorem, an improved finite element model for periodic stiffened plate structures with any number or orientation of stiffeners is developed to describe the propagation of elastic waves in the periodic structures undergoing flexural vibration. Using the finite element model, the flexural vibration band gaps of a periodic grid structure and several periodic stiffened plate structures with different skin thicknesses are compared and analyzed. The results indicate that the vibration coupling between the skin and the stiffeners influences the formation of flexural vibration band gaps.

Keyword: phononic crystals; band gaps; periodic structures; stiffened plates; vibration and noise control.

Received February 17, 2011
Accepted March 08, 2012